Amino acids substitutions in σ1 and μ1 outer capsid proteins of a Vero cell-adapted mammalian orthoreovirus are required for optimal virus binding and disassembly

Véronique Sandekian and Guy Lemay*

Département de microbiologie, infectiologie et immunologie, Université de Montréal, Montréal, Canada H3C 3J7

*Corresponding author: Tel: +1 514 343 2422
Fax: +1 514 343 5701
Email address: guy.lemay@umontreal.ca (G. Lemay)
Département de microbiologie, infectiologie et immunologie
Pavillon Roger-Gaudry, Université de Montréal
P.O. Box 6128, Station Centre-ville
Montréal (Québec), Canada H3C 3J7

Running title: Reovirus adaptation to Vero cells

ABSTRACT

In a recent study, the serotype 3 Dearing strain of mammalian orthoreovirus was adapted to Vero cells; cells that exhibit a limited ability to support the early steps of reovirus uncoating and are unable to produce interferon as an antiviral response upon infection. The Vero cell-adapted virus (VeroAV) exhibits amino acids substitutions in both the σ1 and μ1 outer capsid proteins but no changes in the σ3 protein. Accordingly, the virus was shown not to behave as a classical uncoating mutant. In the present study, an increased ability of the virus to bind at the Vero cell surface was observed and is likely associated with an increased ability to bind onto cell-surface sialic acid residues. In addition, the kinetics of μ1 disassembly from the virions appears to be altered. The plasmid-based reverse genetics approach confirmed the importance of σ1 amino acids substitutions in VeroAV's ability to efficiently infect Vero cells, although μ1 co-adaptation appears necessary to optimize viral infection. This approach of combining *in vitro* selection of reoviruses with reverse genetics to identify pertinent amino acids substitutions appears promising in the context of eventual reovirus modification to increase its potential as an oncolytic virus.

Keywords: Reovirus; Mutants; Binding; Uncoating; Sigma1; Mu1

1. Introduction

Mammalian orthoreoviruses, hereafter referred to as “reovirus”, are prototype members of the *Orthoreovirus* genus in the *Reoviridae* family. These viruses are generally cytolytic as they kill and lyse infected cells in culture; this has been generally attributed to apoptosis (reviewed in: Clarke et al., 2005; Danthi et al., 2010), although both necrotic (Berger and Danthi, 2013) and autophagic (Thirukkumaran et al., 2013) cell death likely occurs in certain cell types.

In the last few years, there has been renewed interest in the study of these viruses, given their ability to discriminate between normal and transformed/cancer cells, specifically infecting and killing the latter and giving rise to the idea of using them as “oncolytic viruses”. This has led to numerous clinical studies as reviewed by others (Black and Morris, 2012; Clements et al., 2014; Harrington et al., 2010; Kelly et al., 2009; Maitra et al., 2012). Despite the fact that reoviruses are naturally oncolytic without prior genetic modifications, there is still a significant research effort ongoing to obtain novel virus variants better adapted to infect, replicate in, and kill cancer cells while sparing non-transformed cells (van den Hengel et al., 2013; Kim et al., 2011; Rudd and Lemay, 2005; Shmulevitz et al., 2012; van den Wollenberg et al., 2009, 2012). One possible approach is to take advantage of novel viral variants that could be selected during establishment of viral persistence in different cell types.

Although reoviruses are considered to be essentially cytolytic, there have been numerous reports of persistence establishment with these viruses upon long-term cultivation of infected cells (reviewed in: Dermody, 1998). Since constant viral reinfection is needed to maintain the infected state, this has led to the identification of viral mutants, but few of those have been well characterized. In the most-studied L929 cell model, various amino acid substitutions were found in the viral σ1 protein and a single amino acid substitution in σ3 (Y354H); both proteins being part of the outer capsid of the virion. The σ3-Y354H substitution was later shown to be most important for the ability of the virus to be maintained in persistently infected cells (Baer and Dermody, 1997; Ebert et al., 2001; Wetzel et al., 1997; Wilson et al., 2002). This amino acid substitution is located at the surface-exposed lobe of the σ3 outer capsid protein, thus increasing the protein's sensitivity to proteases and favoring viral uncoating under conditions where proteases are present in limiting amount (Baer and Dermody, 1997; Wetzel et al., 1997). In more recent studies, amino acid substitutions in σ3 were again observed in viruses recovered from Raji, HT1080 and CA46 cells, at positions consistent with an increased uncoating of these viruses; substitutions in σ1 were also found in two of these viruses (Kim et al., 2011).

In the most recent study on reovirus persistence (Jabre et al., 2013), a novel variant of reovirus serotype 3 Dearing

(T3/Human/Ohio/Dearing/55), named Vero cell-adapted virus (VeroAV) was obtained by long-term culture of the virus on these cells that were previously shown to be somewhat resistant to a wild-type virus, due to their reduced ability to uncoat the virus (Golden et al., 2002). Prior treatment with chymotrypsin, uncoating virions to "infectious subviral particles" (ISVPs), significantly augmented infection by a wild-type virus while VeroAV exhibits an increased ability to infect Vero cells even in the absence of prior uncoating by chymotrypsin treatment. Surprisingly, VeroAV did not behave as an uncoating mutant, still showing normal sensitivity to inhibitors of lysosomal cathepsins, in contrast with uncoating mutants selected during viral persistence in L929 cells (Baer and Dermody, 1997; Wilson et al., 2002). Accordingly, VeroAV does not harbor amino acid substitutions in its σ3 protein (Jabre et al., 2013). However, two amino acids substitutions were found in each of the σ1 and μ1 outer capsid proteins (Jabre et al., 2013), at positions consistent with an altered binding to host cell surface or outer capsid disassembly (Reiter et al., 2011; Zhang et al., 2005), but this was not further studied at the time.

The σ1 protein forms the surface-exposed spikes at the surface of the virion and binds to both sialic acid and the JAM receptor at the cell surface (Danthi et al., 2010; Dermody et al., 2013), σ1 is also retained in infectious subviral particles (ISVPs) that are generated by proteolytic cleavage of the outer capsid proteins; in fact, reovirus uncoating has been shown to increase the binding of the resulting ISVPs to the cell surface (Chappell et al., 1998; Nibert et al., 1995). The proteolytic cleavage of the outer capsid, referred to as "uncoating", takes place in endosomes following endocytosis of the viral particles or in the extracellular milieu where proteases are present. Uncoating can also be achieved in the laboratory by chymotrypsin treatment of virions and this facilitates infection of certain cell types, such as the Vero cells used in the present study, that are inefficient in their ability to uncoat the virus (Golden et al., 2002). During uncoating, the σ3 protein is first removed, followed by proteolytic cleavage of the μ1 protein, allowing the viral particles to cross the cellular or endosomal membrane (Danthi et al., 2010; Dermody et al., 2013). Together, the three outer capsid proteins σ1, σ3 and μ1, are thus critical in infectivity of the viral particles and initiation of the viral replication cycle.

In the present study, the importance of the σ1 and μ1 amino acid substitutions of VeroAV was thus further examined. The virus was first shown to exhibit an increased binding at the surface of Vero cells likely due to an increased binding to cell-surface sialic acid residues. An altered disassembly of its outer capsid, as evidenced by different kinetics of *in vitro* cleavage by chymotrypsin, was also observed. The novel plasmid-based reverse genetics system (Kobayashi et al., 2007, 2010; reviewed in: Boehme et al., 2011; van den Hengel et al., 2013; Lemay, 2011) then allowed to establish that the

preferential infection of Vero cells is actually due to the σ1 amino acid substitutions, although the co-adaptation of μ1 appears necessary to optimize viral infection. Altogether, these results indicate that the establishment of viral persistence can select for different viral variants depending on the cell type. Combined with the analytical tool of reverse genetics, this could allow for the optimization of selective reovirus infection of different cell types.

2. Material and Methods

2.1. Cell lines and viruses

L929, HeLa and Vero cells were originally obtained from the American type culture collection (ATCC); the BHK cells stably expressing the T7 RNA polymerase have been described (Buchholz et al., 1999) and were a generous gift from the laboratory of Dr John Hiscott (Lady Davis Research Institute, Montréal, Canada). All cells were grown in minimal Eagle medium (MEM) with 5% fetal bovine serum. Wild-type reovirus laboratory stock ($T3D^S$) was derived from a pure plaque of reovirus type 3 Dearing (T3/Human/Ohio/Dearing/55) and propagated at low multiplicity of infection on L929 cells. The original inoculum was obtained from the American Type Culture Collection (ATCC). Vero cell-adapted reovirus (VeroAV) was obtained following long-term culture of the wild-type virus on Vero cells (Jabre et al., 2013) and propagated on HeLa cells.

2.2. Antibodies

Hybridoma cell lines producing either anti-σ3 (4F2) or anti-μ1 (10F6) have been described (Virgin et al., 1991) and were obtained from Dr Kevin Coombs (University of Manitoba). Cells were grown in MEM for suspension culture with 10% fetal bovine serum, proline (20μg/ml) and β-mercaptoethanol (50μM) and antibodies were recovered, as previously described (Brochu-Lafontaine and Lemay, 2012). The polyclonal antiserum directed against the carboxyl-terminal head domain of σ1 was produced originally in the laboratory of Dr. Terence Dermody (Vanderbilt University, Tennessee) and was a generous gift from Dr. Earl Brown (University of Ottawa). The rabbit anti-tubulin antiserum was obtained from ICN Biomedicals Inc.

2.3. Determination of virus titer

Virus titers were determined by $TCID_{50}$ method on L929 cells in 96-wells plates (Danis and Lemay, 1993). For electron microscopy, infectious virus stocks were extracted once with Vertrel® XF (1,1,1,2,3,4,4,5,5,5-decafluoropentane; Miller-Stephenson Chemical company Inc.) (Mendez et al., 2000) to remove most cellular debris and mixed with latex beads at a known concentration. Processing of samples and microscopic observations were done at the INRS-Institut Armand Frappier (Laval, Québec) electron microscopy facilities.

2.4. Virus binding at the host-cell surface

Infectious viral particles at a MOI of 80 PFU/cell were allowed to bind onto the host-cell surface of L929 or Vero cells for one hour at 4ºC with occasional gentle agitation. Cells with bound virions were then extensively washed with cold medium and immediately frozen at -80ºC for virus titration. In some experiments, neuraminidase (from *Clostridium perfringens*, New England Biolabs) pretreatment was done at 37ºC at a concentration of 50 units/ml in tissue culture medium for one hour. Neuraminidase was then removed, cells were washed with medium, and binding of virions at 4ºC was performed, as before.

2.5. In vitro cleavage of capsid proteins with chymotrypsin

Virions prepared by Vertrel extraction of viral stocks (propagated in the absence of serum) were incubated from 0 to 30 minutes at 10 or 40 µg/ml concentrations of chymotrypsin at 37ºC or 28ºC. Reactions were stopped by addition of 2 mM phenylmethylsulfonyl fluoride (PMSF) and samples were analyzed by immunoblotting using either the combination of anti-µ1 and anti-σ3 monoclonal antibodies or the anti-σ1 polyclonal antiserum.

2.6. Immunoblotting

Infected cells were recovered by scraping in a small volume of medium and processed for immunoblotting, as previously described (Brochu-Lafontaine and Lemay, 2012). Images were obtained using either autoradiography on Kodak BioMax Light films or on a Typhoon Trio™ imager (GE Healthcare Life Sciences).

2.7. Plasmid constructs

The plasmids separately harboring each of the cDNA corresponding to the 10 genes of reovirus serotype 3 Dearing

(T3D^K), under the transcriptional control of the T7 promoter, were previously described (Kobayashi et al., 2007) and were a generous gift from the laboratory of Dr Terence Dermody (Vanderbilt University, Nashville, Tennessee). To obtain the virus mutant harboring the amino acids substitutions of VeroAV in the defined background of the reverse genetics system, a fragment of the gene encompassing all mutations was obtained by RT-PCR amplification on the viral VeroAV genome, essentially as previously described (Brochu-Lafontaine and Lemay, 2012; Jabre et al., 2013). PCR fragments were recovered and subcloned to replace the corresponding fragment in the M2 or S1 reverse genetics plasmid. A similar strategy was used to construct a wild-type plasmid corresponding to the initial wild-type laboratory virus stock (T3D^S).

2.8. Rescue of infectious mutant viruses by reverse genetics

Small-scale preparations of endotoxin-free plasmid DNA, corresponding to the different M2 and S1 genes were column-purified as recommended by the manufacturer (Zyppy plasmid miniprep kit, Zymo Research). Recovery of infectious reovirus stocks by transfection of the baby hamster kidney (BHK) cell line constitutively expressing the T7 RNA polymerase (Buchholz et al., 1999) was done essentially as previously described (Brochu-Lafontaine and Lemay, 2012). The presence of the expected amino acid substitutions and absence of other mutations on the three genes encoding outer capsid proteins was verified by RT-PCR and sequencing of the corresponding fragment, as for the original VeroAV (Jabre et al., 2013).

2.9. Plaque assay

Plaque assays were performed on Vero cells in the presence of chymotrypsin (Sigma Type I-S from bovine pancreas) at 5μg/ml, as previously described (Brochu-Lafontaine and Lemay, 2012; Jabre et al., 2013).

3. Results

3.1. Binding of reovirus VeroAV at the cell surface

Considering the position of the amino acids substitutions on both σ1 and μ1 of VeroAV, it was previously suggested that virus disassembly and/or binding could be affected by these changes (Jabre et al., 2013). This last point was first examined as a possible explanation for the increased ability of VeroAV to infect Vero cells.

Infectious virus stocks of either VeroAV or the original wild-type laboratory virus stock from which it was

originally derived were thus prepared by infection of HeLa cells; this wild-type virus will be referred to as type 3 Dearing, isolate Sandekian ($T3D^S$) to distinguish it from other stocks of wild-type virus, as will be discussed later in the manuscript. VeroAV and $T3D^S$ virus stocks were first compared to determine if they exhibit a similar particle/infectious titer ratio. The presence of similar numbers of $T3D^S$ and VeroAV viral particles for the same viral titer was confirmed by quantitative electron microscopy using a latex bead standard (data not shown). Although somewhat variable from one preparation to another, the ratio of the number of virus particles to viral infectivity titer was approximately 100 particles/PFU for both viruses. This is, in fact, quite similar to previous reports by other groups (Bokiej and Dermody, 2012; Doyle et al., 2012; Frierson et al., 2012; Hand and Tamm, 1973; Mendez et al., 2000).

To directly determine their binding to the cell surface, virions were then adsorbed onto the cells In a preliminary experiment, binding of the $T3D^S$ virus was shown to increase linearly at all MOI tested, up to 250 (data not shown). This is not surprising considering that binding assay are routinely performed at 50,000 particles per cell by other investigators (for example Bokiej and Dermody, 2012). An intermediate MOI of 80 was thus used thereafter to avoid saturation of the cellular receptors. In these conditions, $T3D^S$ bound to both L929 and Vero cells with essentially the same efficiency whereas the VeroAV virions showed more than fivefold increase in binding to Vero cells compared to the $T3D^S$ virions (Fig. 1). Although VeroAV virions also apparently bind slightly better to the L929 cell surface, this difference was not statistically significant. The data rather indicate that the increase in binding of VeroAV at the cell surface results from an adaption to binding preferentially onto these cells.

3.2. Binding of wild-type $T3D^S$ and VeroAV virions to sialic acids

Considering the position of the amino acid substitutions observed in σ1 of VeroAV (Table I), compared with wild-type $T3D^S$ and wild-type reverse genetics virus (T3D-Kobayashi, $T3D^K$), an increased binding of the virions to sialic acids at the cell surface was postulated. Amino acid 198 is part of the sialic acid binding region of the protein, and is known to somehow contribute to the sialic binding property of the protein (Chappell et al., 1997; Dermody et al., 1990), although it does not appear to directly interact with the sugar moieties (Reiter et al., 2011).

In a preliminary experiment, the hemagglutination potential of VeroAV was examined as a first indication of binding to sialic acid (Chappell et al., 1997; Dermody et al., 1990). Semi-purified viral particles from either $T3D^S$ or VeroAV were submitted to serial twofold dilutions and their ability to agglutinate bovine red blood cells was compared. At the

concentrations used, hemagglutination could not be detected with the semi-purified $T3D^S$ virions while, at the same protein concentration, hemagglutination was observed up to the 4^{th} binary dilution with VeroAV. In this assay, when compared with cesium chloride-purified $T3D^S$ virions, the hemagglutination potential of VeroAV is thus at least 8-fold higher than that of $T3D^S$ (supplementary Fig. S1).

To further determine if the presence of sialic acid at the cell surface is involved in the increased binding of VeroAV to the surface of Vero cells, the cells were pre-treated with neuraminidase to remove cell surface sialic acids before virus binding. In preliminary experiments, the concentration of 50 units/ml appeared as optimal to see an effect on virus adsorption while minimizing host-cell toxicity (data not shown) this concentration was thus retained as experimental conditions. Although not considered statistically significant, an almost twofold increase in binding was found with $T3D^S$; this is somewhat reminiscent of the situation observed with some "sialidase-insensitive" rotavirus strains (Haselhorst et al. 2009). This was not further investigated but could be due to increased accessibility of other cellular receptors, either protein such as the JAM receptor or other glycans, after terminal sialic acid removal by neuraminidase. In contrast, there was an almost threefold decrease in binding for VeroAV under the same conditions (Fig. 2). Altogether these results support the idea that increased binding of VeroAV at the surface of Vero cells depends on the presence of sialic acid residues at the cell surface.

3.3. Outer capsid disassembly of wild-type $T3D^S$ and VeroAV virions

Considering the position of amino acid substitutions on μ1, there is also a possibility that its cleavage and outer capsid disassembly could be affected, as discussed previously (Jabre et al., 2013), and could thus affect the differential infectivity of the virus in the presence or absence of prior chymotrypsin treatment. To directly examine this possibility, virions were treated with 10μg/ml chymotrypsin *in vitro* for different times. As expected, removal of σ3 was observed for both $T3D^S$ and VeroAV, although apparently less efficiently for VeroAV. However, a striking difference was observed for μ1 that was gradually converted from μ1C to δ for $T3D^S$ while μ1C of VeroAV gradually disappeared without concomitant accumulation of δ protein (Fig. 3, upper panel).

This kinetics of $T3D^S$ disassembly is similar to that previously reported for serotype 1 Lang virus (T1L), while that of VeroAV resembles that of $T3D^K$ (Madren et al., 2012; Sarkar and Danthi, 2010). This is not unexpected since the μ1

protein of $T3D^S$ harbors a valine at position 305, as in T1L, while an alanine is found in other isolates of T3D such as $T3D^K$ (Table I). This difference between $T3D^K$ and T1L is responsible for their different disassembly kinetics (Madren et al., 2012). In contrast, although it harbors a valine at position 305, VeroAV behaves as $T3D^K$; this is most likely due to the additional amino acid substitutions at positions 89 and/or 114 (Jabre et al., 2013). Interestingly, while we were completing this work, it has been further established that the loop comprising amino acids 72 to 96 of μ1 is involved in stability of the outer capsid and affects its disassembly upon protease treatment. It is especially striking that glutamic acid 89 was found to be the most critical amino acid in this phenotype (Sarkar and Danthi, 2013).

The amount of σ1 in the viral particles during gradual disassembly was also examined by immunoblotting. There was no apparent difference in the stability of the protein in the viral capsid during disassembly (Fig. 3, lower panel); however, a significantly higher amount of σ1 was found in VeroAV virions compared to $T3D^S$ virions; as estimated by the ratio of σ1 to σ3 signal, there appears to be approximately three times more σ1 per viral particle for VeroAV compared to the $T3D^S$ virions, raising the possibility that the amount of σ1 in the viral particle, in addition to a difference in affinity for sialic acids, could be responsible for increased virus binding at the cell surface.

3.4. Rescue of virus mutants using plasmid-based reverse genetics

To confirm that the amino acid substitutions in σ1 and μ1 are responsible for T3D adaptation to Vero cells and to explore whether amino acid substitutions on both proteins are required, the fragments encompassing the substitutions of VeroAV compared to $T3D^S$ were obtained by RT-PCR on the viral genomic dsRNA and used to substitute the homologous fragment in the corresponding gene of $T3D^K$ used for plasmid-based reverse genetics (Kobayashi et al., 2007).

These plasmid constructs could then be used to generate a mutant virus harboring the amino acid substitutions of VeroAV σ1 (protein referred hereafter as σ1-AV), including those differences between $T3D^S$ and $T3D^K$ that are also present in the same fragment. In parallel, the same procedure was applied to generate a plasmid harboring solely the three amino acid differences between $T3D^S$ and $T3D^K$ in this protein (proteins referred hereafter as σ1-S and σ1-K, respectively), in order to generate a control virus in a $T3D^K$ background for all other viral proteins. A similar procedure was used for the M2 gene to introduce the fragment encompassing all amino acids changes on μ1 of VeroAV, including differences between $T3D^S$ and $T3D^K$ (protein hereafter referred to as μ1-AV). These two amino acid differences between $T3D^S$ and $T3D^K$ were introduced in a separate plasmid to generate a control virus harboring the μ1 protein of $T3D^S$ (hereafter referred to as μ1-S) in a wild-type $T3D^K$ background. The amino acid differences between $T3D^K$, $T3D^S$ and VeroAV in both σ1 and μ1 proteins

are summarized in Table I.

The different plasmids were then used in the plasmid-based reverse genetics system to rescue viruses harboring amino acid substitutions in either σ1, μ1 or both, in an otherwise wild-type $T3D^K$ background. All viruses were propagated before sequencing of the complete genes encoding σ1, σ3 and μ1 of the final virus stocks to confirm that they possessed the expected sequences.

For some viruses, the titers obtained upon viral propagation remained very low (Fig. 4). Interestingly, it appears that viruses produced with μ1-K had higher titers than those with either μ1-S or μ1-AV except for the σ1-AV/μ1-AV combination. The worst combination was that of σ1-AV/μ1-S, strongly suggesting that μ1-S had to evolve concomitantly with σ1-AV during selection of VeroAV.

3.5. Infectivity of rescued viruses in Vero cells

The different viruses were then analyzed for their relative ability to infect Vero cells in the presence or absence of chymotrypsin in a single-cycle assay using immunoblotting. Two viruses, presenting poorly adapted protein combinations (σ1-K with μ1-AV and σ1-AV with μ1-S), and whose titers were reduced more than a thousandfold, were not examined.

As expected, viruses harboring either σ1-S/μ1-S or σ1-K/μ1-K wild-type combinations were poorly infectious on Vero cells in the absence of chymotrypsin while their infectivity was increased upon chymotrypsin treatment (Fig. 5), as with the original wild-type $T3D^S$ virus. The combination σ1-AV/μ1-AV resulted in a virus that was able to infect Vero cells independently of the presence of chymotrypsin, with even a small reduction in its presence, similar to the parental VeroAV. The two proteins are thus solely responsible for the adaptation of VeroAV to better infect Vero cells.

The σ1-AV protein VeroAV combined with μ1-K did confer by itself an ability to promote infection of Vero cells in the absence of chymotrypsin. In contrast μ1-AV by itself had no effect when combined with σ1-S. Altogether, these data indicate that amino acid substitutions in σ1-AV are the primary determinants of the increased ability of VeroAV to infect Vero cells as virions. However, the nature of the μ1 protein is also of importance to optimize virus infection. While the σ1-AV/μ1-S virus could not be further studied, the σ1-AV/μ1-K virus was still partly dependent on prior chymotrypsin treatment to infect Vero cells (Fig. 5), indicating that μ1-AV contributes to overall viral fitness but may also affect the ability of σ1-AV to promote infection of Vero cells.

In contrast to the predominant effect of σ1-AV on infection of Vero cells, the μ1-AV protein appears to be essentially responsible for increased sensitivity to chymotrypsin resulting in smaller plaques (Table II). As previously illustrated (Jabre et al., 2013), wild-type plaques are approximately 0.7 to 1 mm in diameter under the conditions used while VeroAV plaques are mostly punctate and less than 0.2 mm in diameter. The 4 different combinations of $T3D^S$ and $T3D^K$ proteins did not yield plaque sizes that were significantly different from wild-type while the introduction of both σ1-AV and μ1-AV yielded plaques that were similar in size to that of the original VeroAV. However, the sole addition of μ1-AV to either σ1-S or σ1-K resulted in a small-plaque phenotype suggesting that μ1-AV is responsible for this phenotype, as expected from its altered kinetics of chymotrypsin cleavage *in vitro* in the original VeroAV. The exact contribution of σ1-AV to this phenotype was more difficult to assess since it was not fully compatible with other μ1 proteins. However, despite a lower virus titer, plaques were still seen when σ1-AV was combined with μ1-K; their size was intermediate between that of $T3D^S$ and VeroAV plaques. The resistance σ1-AV to *in vitro* chymotrypsin digestion of the parental VeroAV (as shown in Fig. 3, lower panel) also supports the idea that it is not the principal determinant of chymotrypsin sensitivity or of altered virus disassembly.

3.6. Further characterization of rescued $T3D^K$(σ1-AV/μ1-AV)

The phenotypic properties of the rescued virus harboring either the σ1 and μ1 protein of either $T3D^S$ or VeroAV in the $T3D^K$ background were then further examined. First, the effect of neuraminidase treatment on binding to Vero cells was examined by comparing the original $T3D^S$ and VeroAV with the rescued viruses, namely $T3D^K$(σ1-AV/μ1-AV) and $T3D^K$(σ1-S/μ1-S). The results confirmed that the presence of both σ1 and μ1 of VeroAV increased sensitivity to neuraminidase treatment up to a level similar to that of the original VeroAV (Fig.6, panel A). However, the increased binding of $T3D^S$ observed upon neuraminidase treatment was not observed with $T3D^K$(σ1-S/μ1-S). This suggests that other differences between $T3D^S$ and $T3D^K$ do exist in other viral protein(s) and that they indirectly affect the phenotype of σ1, as shown by others with amino acids substitutions in λ2 (Shmulevitz et al. 2012).

The kinetics of *in vitro* proteolytic uncoating of the same two rescued viruses was then examined and compared with that of the original $T3D^S$ and VeroAV, as in figure 3. This time, uncoating was examined at both 37ºC and 28ºC, as described (Sarkar and Danthi, 2013). Removal of σ3 was less efficient for $T3D^K$(σ1-AV/μ1-AV) than for $T3D^K$(σ1-S/μ1-S), as with the original viruses (Fig. 6, panel

B), and this was better evidenced at the lower temperature; this indicates that the different kinetics of uncoating was maintained in the rescued viruses. More importantly, $T3D^K$(σ1-S/μ1-S) showed an almost complete conversion of μ1C to δ at 37ºC, as expected, while in $T3D^K$(σ1-AV/μ1-AV) there was a decline of μ1C without concomitant accumulation of δ. Again, the phenotype of $T3D^K$(σ1-AV/μ1-AV) was thus essentially the same as that of the original VeroAV, in which δ is rapidly removed from ISVPs in the presence of proteases, and the wild-type $T3D^K$(σ1-S/μ1-S) behaves as the original $T3D^S$ virus.

Finally, immunoblotting was performed on viral particles for some of these viruses whose titers were sufficiently high (Fig. 7). It was found that both the sequence of σ1 and μ1 affected the amount of virion-associated σ1. Virions corresponding to plasmid-rescued VeroAV $T3D^K$(σ1-AV/μ1-AV) harbor more σ1 relative to σ3 than virions from plasmid-rescued $T3D^K$(σ1-S/μ1-S), as observed with the original viruses presented on the right panel, as a control. This also corresponds to the previous observation at time 0 on Fig. 3. However, μ1-K was able to increase the amount of both σ1-S and σ1-AV in the virion despite the fact that $T3D^K$ itself harbors a low amount of σ1. This again indicates that a compatibility between μ1 and σ1 is needed to optimize both the incorporation and function of σ1 in the viral particles. However, there was no apparent relation between the number of σ1 molecules incorporated to the virion and either the ability to infect Vero cells (Fig. 5) or the replicative ability of these viruses on HeLa cells used for viral propagation (Fig. 4).

4. Discussion

As with most viruses, the replicative ability of mammalian reoviruses has been mostly examined in few cell types. In the last few years, renewed interest in oncolytic reovirus replication has led to the realization that the nature of the host

cells could restrict viral infection and lead, in return, to virus adaptation. In a previous work (Jabre et al., 2013), Vero cells were chosen as a model; these cells are also classically used to grow viruses for clinical applications (Berry et al., 1999; World Health Organization, 1987) and are deficient in interferon production (Desmyter et al., 1968; Emeny and Morgan, 1979), thus facilitating large-scale production of interferon-sensitive viruses.

Surprisingly, virus persistence of reovirus in Vero cells did not give rise to a virus with an increased ability to be uncoated by lower amount of lysosomal cathepsins following viral endocytosis (Jabre et al., 2013). Accordingly, the σ3 protein, known as the major determinant of reovirus uncoating efficiency was left unaltered in VeroAV. However, the other two other outer capsid proteins, σ1 and μ1, respectively responsible for earlier step of virus binding at the host cell surface and later step of viral disassembly, were both exhibiting amino acids substitutions. Although the position of the substitutions lead to speculate about a possible alteration of virus binding and/or later disassembly steps (Jabre et al. 2013), there was no experimental evidence to support this idea. In the present study, the virus was further studied by the new tools of plasmid-based reverse genetics in order to introduce the VeroAV amino acids substitutions in a wild-type virus background. These studies allowed to firmly establish that the σ1 and μ1 amino acids substitutions are solely responsible for the ability of VeroAV to infect Vero cells in the absence of prior uncoating while giving rise to viruses that are more readily inactivated upon prolonged protease treatment. The increased ability to infect Vero cells was assigned essentially to an increased binding to sialic acids, as previously hypothesized (Jabre et al. 2013); however, a very interesting point is the apparent co-evolution between σ1 and μ1, suggesting that these two proteins need to be well-adapted to each other in order to optimize viral fitness.

If binding at the cell surface is critical to the efficient infection of Vero cells by VeroAV, it may appear surprising that the wild-type viruses can attach at similar levels on L929 and Vero cells; however, this is consistent with previous observations showing that binding of wild-type ISVPs is not increased compared to virions on Vero cells, despite the increase in infection (Golden et al., 2002). It is possible that the increased binding of VeroAV virions rather contributes to facilitate later entry steps, normally bypassed in ISVPs. Asparagine 198 was previously shown to be involved in σ1 binding

to sugars containing sialic acid (Chappell et al., 1997; Dermody et al., 1990; Reiter et al., 2011), although crystallographic analysis failed to reveal a direct interaction between this amino acid residue and the sugar moieties (Reiter et al., 2011). In these studies, replacing the uncharged asparagine by an acidic amino acid (aspartic acid) was shown to preclude sialic acid binding. Reciprocally, in VeroAV, replacing asparagine by a basic amino acid (lysine) increases sialic acid binding. The observation that N198K was already found early in the process of viral adaptation (Jabre et al., 2013) pleads in favor of its prominent role in the phenotype on Vero cells. However, the virus harboring solely this substitution was only partially able to bypass the restriction in Vero cells and still exhibited reduced infectivity (data not shown), indicating that later amino acids substitutions were required to achieve optimal infection as in VeroAV. Furthermore, it cannot be excluded that some other changes were later selected due to gradual virus-cell coevolution, as observed during reovirus persistence of various cell types (reviewed by: Dermody, 1998).

Unexpectedly, an approximately threefold increase in the amount of σ1 in VeroAV virions compared to the wild-type was observed in the course of this work, and was shown to depend on both the nature of the σ1 and μ1 proteins. However, the increased amount of σ1 per se does not increase infectivity on Vero cells in the absence of adequate amino acid substitutions. It has been reported that some reovirus strains such as type 3 Dearing harbors an average of approximately 18 trimers of σ1 per particle while type 1 Lang harbors a full complement of 36 trimers (Coombs, 1998; Larson et al., 1994); considering the relative difficulty of precisely comparing these results, they appear consistent with a threefold increase in the amount of σ1 that was observed in VeroAV, rendering it similar to T1L with probably the highest possible number of σ1 trimers. It is interesting to note that reducing trimers to only three copies does not seem to affect infectivity, at least in L929 cells (Larson et al., 1994); the lack of effect on viral infectivity on Vero cells when the number of wild-type σ1 trimers increased is also consistent with this idea. Interestingly, an approximately 3-fold difference in σ1 incorporation between two viral clones of reovirus type 3 Dearing was also recently reported (Nygaard et al., 2013) and attributed to an amino acid substitution in the virion-anchoring region of σ1. In VeroAV, the substitution at position 78 is outside the critical 28 amino acid amino-terminal anchoring region; although it cannot be excluded that this substitution in the adjacent region may influence incorporation (Leone et al., 1991). The exact significance of these variations in the amount of virion-incorporated σ1, if any, remains to be established but is likely due to differences in the structural stability of the capsid (Coombs, 1998). This is also supported by the observation that the loss of σ1 upon long-term storage of the virion at 4ºC is more drastic in strains that already have a lower amount of σ1 per virion (Nygaard et al., 2013).

Although the amino acid substitutions in μ1 do not appear to be directly involved in the ability of VeroAV to infect

Vero cells, the nature of the μ1 protein does affect viral replication per se and ability to infect Vero cells in the presence of the σ1 protein of VeroAV. The apparent co-evolution of σ1 and μ1 suggests that these two proteins need to be well-adapted to each other in order to optimize viral fitness. Similar observations were previously made in different contexts such as the determinants of apoptosis or neurovirulence (Clarke et al., 2001; Derrien et al., 2003; Hrdy et al., 1982; Rodgers et al., 1997; Tyler et al., 1996). These μ1 changes selected in VeroAV were probably necessary due to the nature of the μ1 protein in the initial wild-type virus ($T3D^S$) since other μ1 sequences such as that of $T3D^K$ are also able, although not as efficiently, to accommodate the σ1 protein of VeroAV. As previously discussed (Jabre et al., 2013), the contact regions between μ1 in neighboring heterohexamers are similar to the contact regions between μ1 and the λ2 turret protein suggesting that amino acids at this interface, such as amino acid 89, could affect association or exposure of σ1 at the virion's surface (Liemann et al., 2002; Zhang et al., 2005; Middleton et al., 2007). The data presented herein give further support to the idea that these two proteins functionally interact.

The presence of a valine at position 305 of μ1 in both $T3D^S$ and VeroAV also deserves to be further stressed; as previously noted, most isolates of mammalian reoviruses harbor a valine while an alanine is found in some virus stocks such as $T3D^K$. This amino acid was recently shown to affect autocleavage and viral disassembly (Madren et al., 2012; Sarkar and Danthi, 2010) and this difference could explain why the reverse genetics viruses harboring the μ1-K protein are able to promote infection in the absence of chymotrypsin when combined with the σ1-AV protein while the original μ1-S is not. Thus, there is clearly an influence of the original sequence of the virus on the final result obtained upon viral adaptation to a given cell line. Although it is difficult to predict how a virus having a different μ1, such as $T3D^K$, would have evolved under the same conditions, it is likely that either σ1 alone or σ1 and μ1 would have adapted to Vero cells since $T3D^K$ virions infect these cells poorly.

In the present and previous manuscript (Jabre et al., 2013), Vero cells were used to demonstrate that it is possible to generate novel reoviruses that are adapted to different cell lines and that this does not solely rely on the ability of the virus to be uncoated, as in the classical L929 cells model. These proof of concept experiments suggest that it should be also possible to adapt the virus to different cell types in order to further optimize reovirus oncolytic ability. This idea has been previously suggested and, accordingly, novel viruses were found to be better adapted as oncolytic agents (Kim et al., 2011;

Rudd et al., 2005; Shmulevitz et al., 2012; van den Wollenberg et al., 2012). Viruses selected for their large-plaque phenotype using L929 cells, somewhat reminiscent of larger plaques formed by VeroAV on Vero cells in the absence of chymotrypsin, were shown to be better oncolytic viruses both *in vitro* and in animal models (Shmulevitz et al., 2012). A recent report (van den Wollenberg et al., 2012) also suggests that the ability to infect cells independently of the JAM receptor, possibly due to increased binding to sialic acids, could be a useful strategy against cancer cell types that express low levels of JAM and are thus relatively resistant to reovirus (van den Hengel et al., 2013; van den Wollenberg et al., 2009; van Houdt et al., 2008). Furthermore, a virus harboring a deletion of the JAM binding domain and binding solely onto cell surface sialic acids, was shown to be attenuated in nontransformed cells while retaining an oncolytic potential and exhibiting reduced host toxicity (Kim et al., 2011). Although there is no evidence yet that VeroAV has a superior oncolytic activity, it will thus be of interest to further study its ability to lyse tumor cells in tissue culture and eventually in animal models. Novel variant viruses, such as VeroAV, combined with the use of reverse genetics could allow the design of superior oncolytic agents while getting fundamental knowledge on the viral and cellular factors that determine a successful reovirus infection.

Acknowledgments

We thank Dr Takeshi Kobayashi and Dr Terence Dermody (Vanderbilt University, Nashville, Tennessee) for their generous gift of the plasmids used for reverse genetics. We thank Simon Léveillé and Dr John Hiscott (Lady Davis Research Institute, Montreal, Canada) for the initial stock of BHK cells expressing the T7 RNA polymerase, Dr Kevin Coombs (University of Manitoba) for the hybridoma cells producing antireovirus monoclonal antibodies and Dr Earl G. Brown (Ottawa University) for the anti-σ1 polyclonal antiserum originally obtained from Dr Terence Dermody (Vanderbilt University). We thank Miguel Chagnon (Département de Mathématiques et Statistiques, Université de Montréal) for his help with statistical analysis and interpretation.

This work was supported by an operating grant from the Natural Sciences and Engineering Research Council of Canada (NSERC) to G.L. We thank the “Faculté des études supérieures et postdoctorales” of the “Université de Montréal” for partial financial support to V.S.

We thank Roland Jabre for numerous helpful discussions and Dr George Szatmari (Université de Montréal) for critical reading and very helpful suggestions to improve the manuscript.

References

Baer, G.S., Dermody, T.S., 1997. Mutations in reovirus outer-capsid protein sigma3 selected during persistent infections of L cells confer resistance to protease inhibitor E64. J. Virol. 71, 4921–4928.

Berger, A.K., Danthi, P., 2013. Reovirus activates a caspase-independent cell death pathway. MBio 4, e00178.

Berry, J.M., Barnabé, N., Coombs, K.M., Butler, M., 1999. Production of reovirus type-1 and type-3 from Vero cells grown on solid and macroporous microcarriers. Biotechnol. Bioeng. 62, 12–19.

Black, A.J., Morris, D.G., 2012. Clinical trials involving the oncolytic virus, reovirus: Ready for prime time? Expert Rev. Clin. Pharmacol. 5, 517–520.

Boehme, K.W., Ikizler, M., Kobayashi, T., Dermody, T.S., 2011. Reverse genetics for mammalian reovirus. Methods 55, 109–113.

Bokiej, M., Dermody, T.S., 2012. Optimum length and flexibility of reovirus attachment protein sigma1 are required for efficient viral infection. J. Virol. 19, 10270–10280.

Brochu-Lafontaine, V., Lemay, G., 2012. Addition of exogenous polypeptides on the mammalian reovirus outer capsid using reverse genetics. J. Virol. Methods 179, 342–350.

Buchholz, U.J., Finke, S., Conzelmann, K.K., 1999. Generation of bovine respiratory syncytial virus (BRSV) from cDNA: BRSV NS2 is not essential for virus replication in tissue culture, and the human RSV leader region acts as a functional BRSV genome promoter. J. Virol. 73, 251–259.

Chappell, J.D., Gunn, V.L., Wetzel, J.D., Baer, G.S., Dermody, T.S., 1997. Mutations in type 3 reovirus that determine binding to sialic acid are contained in the fibrous tail domain of viral attachment protein σ1. J. Virol. 71, 1834–1841.

Chappell, J.D., Barton, E.S., Smith, T.H., Baer, G.S., Duong, D.T., Nibert, M.L., Dermody, T.S., 1998. Cleavage susceptibility of reovirus attachment protein sigma1 during proteolytic disassembly of virions is determined by a sequence polymorphism in the sigma1 neck. J. Virol. 72, 8205–8213.

Clarke, P., Meintzer, S.M., Widmann, C., Johnson, G.L., Tyler, T.S., 2001. Reovirus infection activates JNK and the JNK-dependent transcription factor c-Jun. J. Virol. 75, 11275–11283.

Clarke, P., Richardson-Burns, S.M., DeBiasi, R.L., Tyler, K.L., 2005. Mechanisms of apoptosis during reovirus infection. Curr. Top. Microbiol. Immunol. 289, 1–24.

Clements, D., Helson, E., Gujar, S.A., Lee, P.W.K., 2014. Reovirus in cancer therapy: an evidence-based review. Oncolytic Virother. 3, 69–82.

Coombs, K.M., 1998. Stoichiometry of reovirus structural proteins in virus, ISVP, and core particles. Virology 243, 218–228.

Danis, C., Lemay, G., 1993. Protein synthesis in different cell lines infected with orthoreovirus serotype 3: inhibition of host-cell protein synthesis correlates with accelerated viral multiplication and cell killing. Biochem. Cell Biol. 71, 81–85.

Danthi, P., Guglielmi, K.M., Kirchner, E., Mainou, B., Stehle, T., Dermody, T.S., 2010. From touchdown to transcription: the reovirus cell entry pathway. Curr. Top. Microbiol. Immunol. 343, 91–119.

Dermody, T.S., Nibert, M.L., Bassel-Duby, R., Fields, B.N., 1990. A σ1 region important for hemagglutination by serotype 3 reovirus strains. J. Virol. 64, 5173–5176.

Dermody, T.S., 1998. Molecular mechanisms of persistent infection by reovirus. Curr. Top. Microbiol. Immunol. 233, 1–22.

Dermody, T.S., Parker, J.S.L., Sherry, B., 2013. Orthoreoviruses, in: Knipe, D.M., Howley, P.M., (Eds.), Fields Virology, 6th Edition. Lippincott, Williams & Wilkins, Philadephia, U.S.A., pp. 1305–1391.

Derrien, M., Hooper, J.W., Fields, B.N., 2003. The M2 gene segment is involved in the capacity of reovirus type 3 Abney to induce the oily fur syndrome in neonatal mice, a S1 gene segment-associated phenotype. Virology 305, 25–30.

Desmyter, J., Melnick, J.L., Rawls, W.E., 1968. Defectiveness of interferon production and of rubella virus interference in a line of African green monkey kidney cells (Vero). J. Virol. 2, 955–961.

Doyle, J.D., Danthi, P., Kendall, E.A., Ooms, L.S., Wetzel, J.D., Dermody, T.S., 2012. Molecular determinants of proteolytic disassembly of the reovirus outer capsid. J. Biol. Chem. 287, 8029–8038.

Ebert, D.H., Wetzel, J.D., Brumbaugh, D.E., Chance, S.R., Stobie, L.E., Baer, G.S., Dermody, T.S., 2001. Adaptation of reovirus to growth in the presence of protease inhibitor E64 segregates with a mutation in the carboxy terminus of viral outer-capsid protein sigma3. J. Virol. 75, 3197–3206.

Emeny, J.M., Morgan, M.J., 1979. Regulation of the interferon system: evidence that Vero cells have a genetic defect in interferon production. J. Gen. Virol. 43, 247–252.

Frierson, J.M., Pruijssers, A.J., Konopka, J.L., Reiter, D.M., Abel, T.W., Stehle, T., Dermody, T.S., 2012. Utilization of sialylated glycans as coreceptors enhances the neurovirulence of serotype 3 reovirus. J. Virol. 86, 13164–13173.

Golden, J.W., Linke, J., Schmechel, S., Thoemke, K., Schiff, L.A., 2002. Addition of exogenous protease facilitates reovirus

infection in many restrictive cells. J. Virol. 76, 7430–7443.

Hand, R., Tamm, I., 1973. Reovirus: effect of noninfective viral components on cellular deoxyribonucleic acid synthesis. J. Virol. 11, 223–231.

Harrington, K.J., Vile, R.G., Melcher, A., Chester, J., Pandha, H.S., 2010. Clinical trials with oncolytic reovirus: Moving beyond phase I into combinations with standard therapeutics. Cytokine Growth Factor Rev. 21, 91–98.

Haselhorst, T., Fleming, F.E., Dyason, J.C., Hartnell, R.D., Yu, X., Holloway, G., Santegoets, K., Kiefel, M.J., Blanchard, H., Coulson, B.S., von Itzstein, M., 2009. Sialic acid dependence in rotavirus host cell invasion. Nat. Chem. Biol. 5, 91–93.

Hrdy, D.B., Rubin, D.H., Fields, B.N., 1982. Molecular basis of reovirus neurovirulence: role of the M2 gene in avirulence. Proc. Natl. Acad. Sci. U.S.A. 79, 1298–1302.

Jabre, R., Sandekian, V., Lemay, G., 2013. Amino acid substitutions in σ1 and μ1 outer capsid proteins are selected during mammalian reovirus adaptation to Vero cells. Virus Res. 176, 188–198.

Kelly, K., Nawrocki, S., Mita, A., Coffey, M., Giles, F.J., Mita, M., 2009. Reovirus-based therapy for cancer. Expert Opin. Biol. Ther. 9, 817–830.

Kim, M., Garant, K.A., zur Nieden, N.I., Alain, T., Loken, S.D., Urbanski, S.J., Forsyth, P.A., Rancourt, D.E., Lee, P.W., Johnston, R.N., 2011. Attenuated reovirus displays oncolysis with reduced host toxicity. Br. J. Cancer 104, 290–299.

Kobayashi, T., Antar, A.A., Boehme, K.W., Danthi, P., Eby, E.A., Guglielmi, K.M., Holm, G.H., Johnson, E.M., Maginnis, M.S., Naik, S., Skelton, W.B., Wetzel, J.D., Wilson, G.J., Chappell, J.D., Dermody, T.S., 2007. A plasmid-based reverse genetics system for animal double-stranded RNA viruses. Cell Host Microbe 1, 147–157.

Kobayashi, T., Ooms, L.S., Ikizler, M., Chappell, J.D., Dermody, T.S., 2010. An improved reverse genetics system for mammalian orthoreoviruses. Virology 398, 194–200.

Larson, S.M., Antczak, J.B., Joklik, W.K., 1994. Reovirus exists in the form of 13 particle species that differ in their content of protein sigma1. Virology 201, 303–311.

Lemay, G., 2011. La génétique inverse dans l'étude des réovirus : progrès, obstacles et développements futurs [Reverse genetics in the study of reoviruses: progress, obstacles and future developments] Virologie 15, 53-62 [in French].

Leone, G., Mah, D.C., Lee, P.W., 1991. The incorporation of reovirus cell attachment protein sigma 1 into virions requires the N-terminal hydrophobic tail and the adjacent heptad repeat region. Virology 182, 346–350.

Liemann, S., Chandran, K., Baker, T.S., Nibert, M.L., Harrison, S.C., 2002. Structure of the reovirus membrane-penetration protein, Mu1, in a complex with is protector protein, Sigma3. Cell 108, 283–295.

Madren, J.A., Sarkar, P., Danthi, P., 2012. Cell entry-associated conformational changes in reovirus particles are controlled by host protease activity. J. Virol. 86, 3466–3473.

Maitra, R., Ghalib, M.H., Goel, S., 2012. Reovirus: a targeted therapeutic – progress and potential. Mol. Cancer Res. 10, 1514–1525.

Mendez, I.I., Hermann, L.L., Hazelton, P.R., Coombs, K.M., 2000. A comparative analysis of freon substitutes in the purification of reovirus and calicivirus. J. Virol. Methods 90, 59–67.

Middleton, J.K., Agosto, M.A., Severson, T.F., Yin, J., Nibert, M.L., 2007. Thermostabilizing mutations in reovirus outer-capsid protein mu1 selected by heat inactivation of infectious subvirion particles. Virology 361, 412–425.

Nibert, M.L., Chappell, J.D., Dermody, T.S., 1995. Infectious subvirion particles of reovirus type 3 Dearing exhibit a loss in infectivity and contain a cleaved sigma 1 protein. J. Virol. 69, 5057–5067.

Nygaard, R.M., Lahti, L., Boehme, K.W., Ikizler, M., Doyle, J.D., Dermody, T.S., Schiff, L.A., 2013. Genetic determinants of reovirus pathogenesis in a murine model of respiratory infection. J. Virol. 87, 9279–9289.

Reiter, D.M., Frierson, J.M., Halvorson, E.E., Kobayashi, T., Dermody, T.S., Stehle, T., 2011. Crystal structure of reovirus attachment protein σ1 in complex with sialylated oligosaccharides. PLoS Pathog. 7, e1002166.

Rodgers, S.E., Barton, E.S., Oberhaus, S.M., Pike, B., Gibson, C.A., Tyler, K.L., Dermody, T.S., 1997. Reovirus-induced apoptosis of MDCK cells is not linked to viral yield and is blocked by Bcl-2. J. Virol. 71, 2540–2546.

Rudd, P., Lemay, G., 2005. Correlation between interferon sensitivity of reovirus isolates and ability to discriminate between normal and Ras-transformed cells. J. Gen. Virol. 86, 1489–1497.

Sarkar, P., Danthi, P., 2010. Determinants of strain-specific differences in efficiency of reovirus entry. J. Virol. 84, 12723–12732.

Sarkar, P., Danthi, P., 2013. The mu1 72-96 loop controls conformational transitions during reovirus cell entry. J. Virol. 87, 13532–13542.

Shmulevitz, M., Gujar, S.A., Ahn, D.G., Mohamed, A., Lee, P.W.K., 2012. Reovirus variants with mutations in S1 and L2 genome segments exhibit enhanced virion infectivity and superior oncolysis. J. Virol. 86, 7403–7413.

Thirukkumaran, C.M., Shi, Z.Q., Luider, J., Kopciuk, K., Gao, H., Bahlis, N., Neri, P., Pho, M., Stewart, D., Mansoor, A., Morris, D.G., 2013. Reovirus modulates autophagy during oncolysis of multiple myeloma. Autophagy 9, 59–58.

Tyler, K.L., Squier, M.K.T., Brown, A.L., Pike, B., Willis, D., Oberhaus, S.M., Dermody, T.S., Cohen, J., 1996. Linkage between reovirus-induced apoptosis and inhibition of cellular DNA synthesis: role of the S1 and M2 genes. J. Virol. 70, 7984–7991.

van den Hengel, S.K., Dautzenberg I.J.C., van den Wollenberg, D.J.M., Sillevis Smitt, P.A.E., Hoeben, R.C., 2013. Genetic modification in mammalian orthoreoviruses, in: Bridgen, A., (Ed.), Reverse genetics of RNA viruses: Applications and perspectives. John Wiley & Sons Ltd., Chichester, West Sussex, UK, pp. 289–317.

van den Wollenberg, D.J., Van Den Hengel, S.K., Dautzenberg, I.J., Kranenburg, O., Hoeben, R.C., 2009. Modification of mammalian reoviruses for use as oncolytic agents. Expert Opin. Biol. Ther. 9, 1509–1520.

van den Wollenberg, D.J.M., Dautzenberg, I.J.C., van den Hengel, S.K., Cramer, S.J., de Groot, R.J., Hoeben, R.C., 2012. Isolation of reovirus T3D mutants capable of infecting human tumor cells independent of junction adhesion molecule-A. PLoS One 7, e48064.

van Houdt, W.J., Smakman, N., van den Wollenberg, D.J.M., Emmink, B.L., Veenendaal, L.M., van Diest ,P.J., Hoeben, R.C., Borel Rinkes, I.H.M., Kranenburg, O., 2008. Transient infection of freshly isolated human colorectal tumor cells by reovirus T3D intermediate subviral particles. Cancer Gene Ther. 15, 284–292.

Virgin, H.W., Mann, M.A., Fields, B.N., Tyler, K.L., 1991. Monoclonal antibodies to reovirus reveal structure/function relationships between capsid proteins and genetics of susceptibility to antibody action. J. Virol. 65, 6772–6781.

Wetzel, J.D., Wilson, G.J., Baer, G.S., Dunnigan, L.R., Wright, J.P., Tang, D.S., Dermody, T.S., 1997. Reovirus variants selected during persistent infections of L cells contain mutations in the viral S1 and S4 genes and are altered in viral disassembly. J. Virol. 71, 1362–1369.

Wilson, G.J., Nason, E.L., Hardy, C.S., Ebert, D.H., Wetzel, J.D., Venkataram Prasad, B.V., Dermody, T.S., 2002. A single mutation in the carboxy terminus of reovirus outer-capsid protein sigma 3 confers enhanced kinetics of sigma 3 proteolysis, resistance to inhibitors of viral disassembly, and alterations in sigma 3 structure. J. Virol. 76, 9832–9843.

World Health Organization., 1987. Requirements for continuous cell lines used for biological substances. World Health

Organ. Tech. Rep. Ser. 745, 99–115.

Zhang, X., Ji, Y., Zhang, L., Harrison, S.C., Marinescu, D.C., Nibert, M.L., Baker, T.S., 2005. Features of reovirus outer capsid protein mu1 revealed by electron cryomicroscopy and image reconstruction of the virion at 7.0 Angstrom resolution. Structure 13, 1545–1557.

Figure legends

Fig. 1. Virus binding at the cell surface. Inoculum of 8 X 10^8 $TCID_{50}$ units of the original wild-type T3D ($T3D^S$) or of the derived Vero cell-adapted virus (VeroAV) were adsorbed at the surface of either L929 or Vero cells at a multiplicity of infection of 80 $TCID_{50}$ units/cell. Following binding for one hour at 4ºC, cells were washed and bound virus was quantitated by $TCID_{50}$ titration on L929 cells. Results are presented as the mean of 5 (L929 cells) and 8 (Vero cells) independent binding experiments. Error bars represent standard error of the mean. P-value are based on a linear mixed-effects model using a random intercept grouped by replica. N.S.: not statistically significant, $p > 0.05$

Fig. 2. Effect of sialic acid removal on virus binding. Vero cells were left untreated or pre-treated with neuraminidase, before adsorption of 2 X 10^8 $T3D^S$ or VeroAV virions and quantitation of bound virus, as in figure 1. Results are presented as the mean of four independent binding experiments with error bars representing standard error of the mean. P-value are based on a linear mixed-effects model using a random intercept grouped by replica. N.S.: not statistically significant, $p > 0.05$

Fig. 3. *In vitro* proteolytic cleavage of outer capsid proteins. Virions from infectious stocks of $T3D^S$ or VeroAV were extracted with Vertrel™ and treated for the indicated times at 37ºC with 10µg/ml chymotrypsin, as described in Methods. Reactions were stopped and proteins analyzed by immunoblotting using combination of anti-σ3 and anti-µ1 monoclonal antibodies (upper panel) or polyclonal antiserum against σ1 (lower panel). Positions of viral capsid proteins are indicated by arrows.

Fig. 4. Replicative ability of rescued viruses. HeLa cells were infected at a MOI of 2 $TCID_{50}$ units/cell and virus stocks obtained by freeze-thaw lysate 48 hours post-infection. Virus titers were obtained by $TCID_{50}$ on L929 cells. Results are

presented relative to the titer obtained with the $T3D^K$(σ1-S/μ1-S) combination (7 X 10^7 PFU/ml) that was arbitrarily fixed to 1.

Fig. 5. Infection of Vero cells with rescued viruses. Viruses obtained by reverse genetics were used to infect Vero cells at a MOI of 2 in the absence or presence of chymotrypsin, as indicated; L929 cells were used as control. Proteins were recovered 24 hours post-infection and analyzed by immunoblotting using a combination of anti-σ3 and anti-μ1 monoclonal antibodies; positions of σ3 and μ1C are indicated. Lower panels present the same membrane that was re-probed with rabbit anti-tubulin antiserum indicating similar amount of proteins in each lane. Infections with the original $T3D^S$ and VeroAV are presented as controls.

Fig. 6. Phenotypic properties of rescued $T3D^K$(σ1-AV/μ1-AV). Vero cells were left untreated or pre-treated with neuraminidase, as in figure 2, before adsorption of $T3D^K$, VeroAV, rescued $T3D^K$(σ1-S/μ1-S) or rescued $T3D^K$(σ1-AV/μ1-AV) at a multiplicity of infection of 80 $TCID_{50}$ units/cell. Following binding for one hour at 4ºC, cells were washed and bound virus was quantitated by $TCID_{50}$ titration on L929 cells, as in figure 1 and 2. The average effect of neuraminidase in two representative experiments is presented with error bars representing standard error of the mean (panel A). Virions from original $T3D^S$ and VeroAV (upper panel) or rescued $T3D^K$(σ1-S/μ1-S) and $T3D^K$(σ1-AV/μ1-AV) were extracted with Vertrel™ and treated for the indicated times at either 28ºC or 37ºC with chymotrypsin, a control reaction was left at 4ºC (panel B). Reactions were stopped and proteins analyzed by immunoblotting using combination of anti-σ3 and anti-μ1 monoclonal antibodies. Positions of σ3 and μ1C and δ proteins are indicated by arrowheads.

Fig. 7. Amount of σ1 in virions of rescued viruses. Infectious virus stocks were extracted once with Vertrel and proteins analyzed by immunoblotting using a combination of anti-σ3 and anti-μ1 monoclonal antibodies (upper panels) or the anti-σ1 polyclonal antiserum (lower panels); positions of σ3, μ1C and σ1 are indicated. The original $T3D^S$ and VeroAV are presented as controls.

Supplementary

Figure legend

Fig. S1. Hemagglutination potential of VeroAV compared to the $T3D^S$. Virus stocks were extracted once with Vertrel to remove most of cellular debris and concentrated by ultrafiltration using Sartorius Vivaspin Turbo 15 centrifugal concentrators (molecular weight cutoff of 1 000 kDa). Serial binary dilution was done in tissue culture medium without serum, starting from an initial titer of 2×10^9 $TCID_{50}$ units/ml. As a control, cesium-chloride purified virus was first diluted 10-fold to reach an infectious titer of approximately 10^{10} $TCID_{50}$ units/ml and similarly subjected to serial binary dilution. Fifty microliters of viruses at different dilutions were placed in round-bottom 96-wells microplates. Washed 10% bovine red blood cells (Cedarlane) were diluted to 1.5% in tissue culture medium and 50µl were added to each well. Plates were examined and photographed after 3 hours of incubation at 4ºC.

Table 1

Table 1:

	$T3D^S$	$T3D^K$	VeroAV	Amino acid position
σ1	Q	Q	P	78
	N	N	K	198
	I	T	I	249
	S	Y	S	253
	A	T	A	408
μ1	E	E	G	89
	A	A	V	114
	V	A	V	305
	T	A	T	449

Differences between the original reverse genetics wild-type clone $T3D^K$ and both the laboratory wild-type virus stock $T3D^S$ and VeroAV are indicated by light gray boxes. Substitutions unique to VeroAV are indicated by dark gray boxes.

Table 2

Table 2:

	σ1-S	σ1-K	σ1-AV
μ1-S	large	large	(-)
μ1-K	large	large	reduced
μ1-AV	small	small	small

Plaque size of rescued viruses. Plaque assays were performed on Vero cells in the presence of chymotrypsin, as described in Materials and methods. Examination of representative plaques 4 days post-infection was done after staining and under an inverted microscope. Large and small plaques were previously illustrated (Jabre et al., 2013); reduced plaques have an intermediate phenotype while (-) indicates the lack of visible plaques.

Figure 1

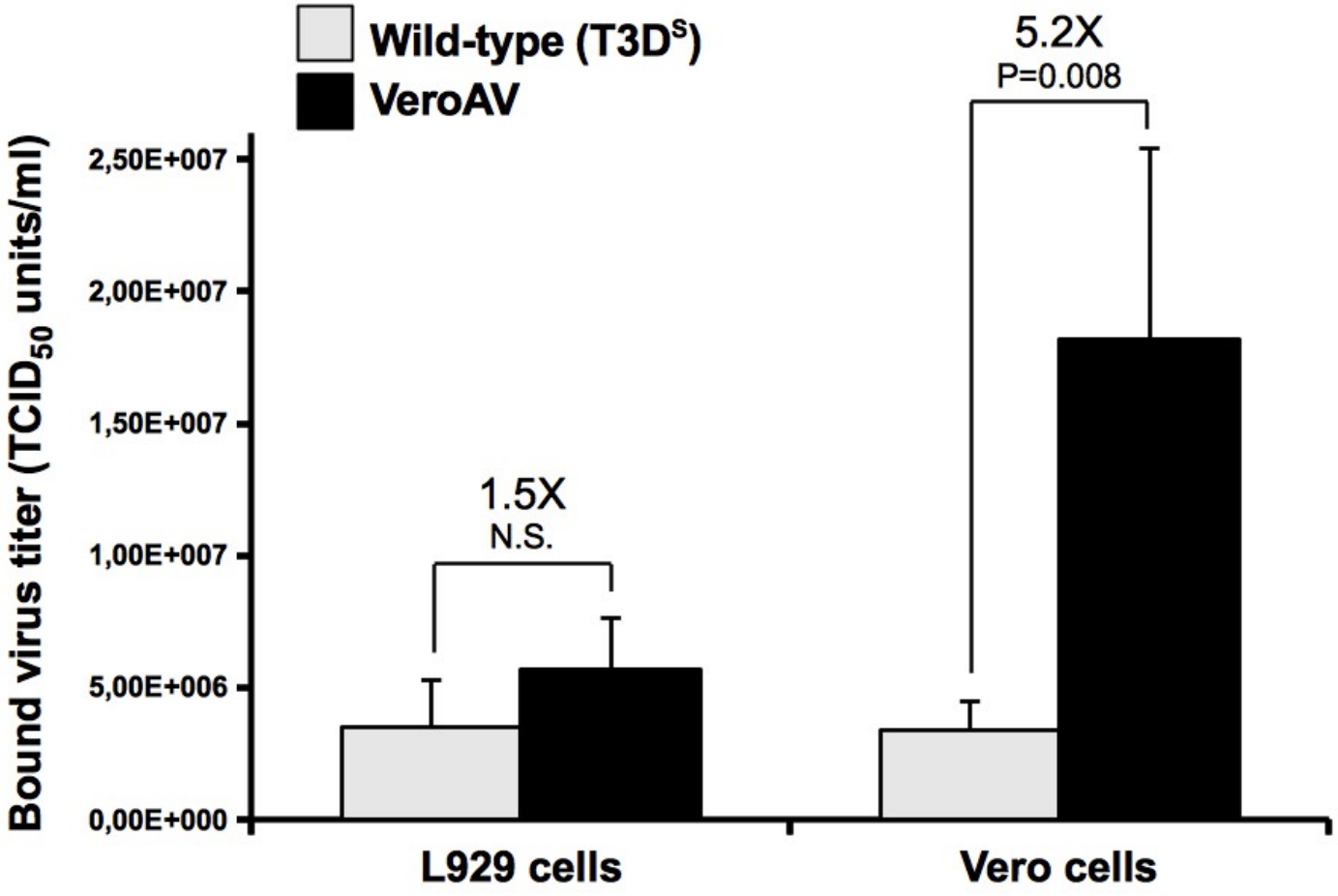
Wild-type (T3D^S)
VeroAV
Bound virus titer (TCID$_{50}$ units/ml)
2,50E+007
2,00E+007
1,50E+007
1,00E+007
5,00E+006
0,00E+000
1.5X
N.S.
5.2X
P=0.008
L929 cells
Vero cells

Figure 2

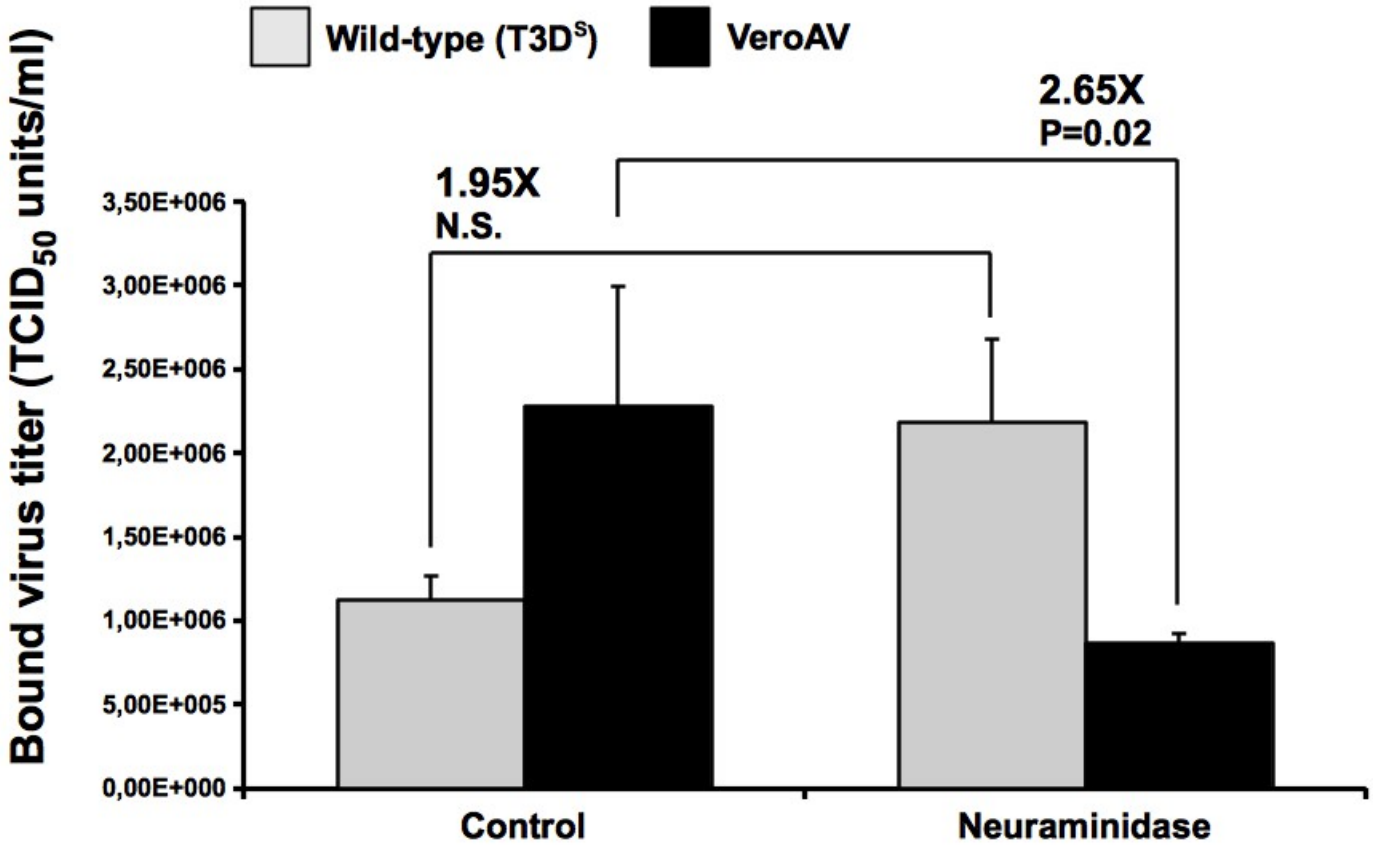
Wild-type (T3D^S)
VeroAV
2.65X
P=0.02
1.95X
N.S.
Bound virus titer (TCID$_{50}$ units/ml)
3,50E+006
3,00E+006
2,50E+006
2,00E+006
1,50E+006
1,00E+006
5,00E+005
0,00E+000
Control
Neuraminidase

Figure 3

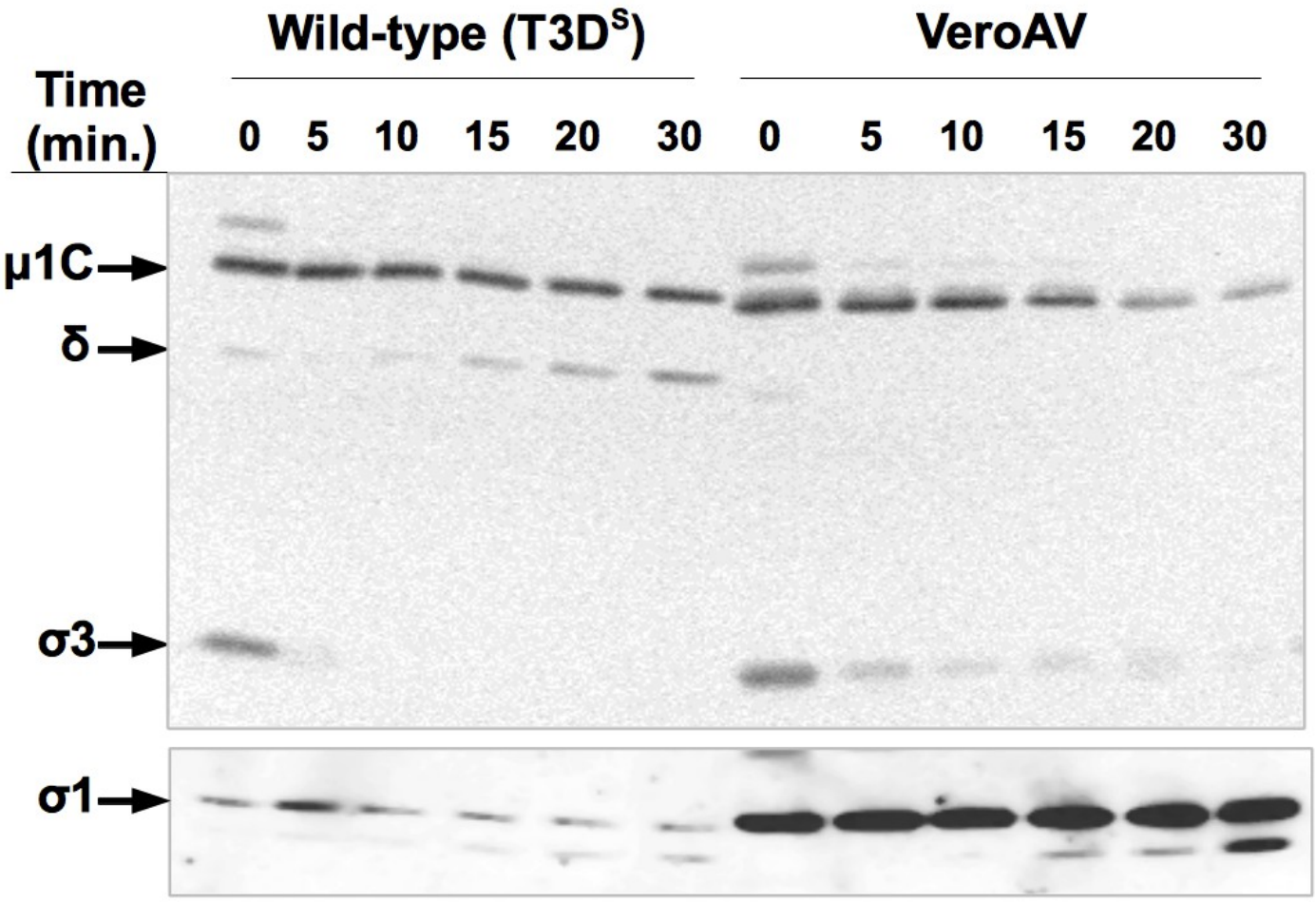
Wild-type (T3D^S)
VeroAV
Time (min.)
0 5 10 15 20 30 0 5 10 15 20 30
μ1C
δ
σ3
σ1

Figure 4

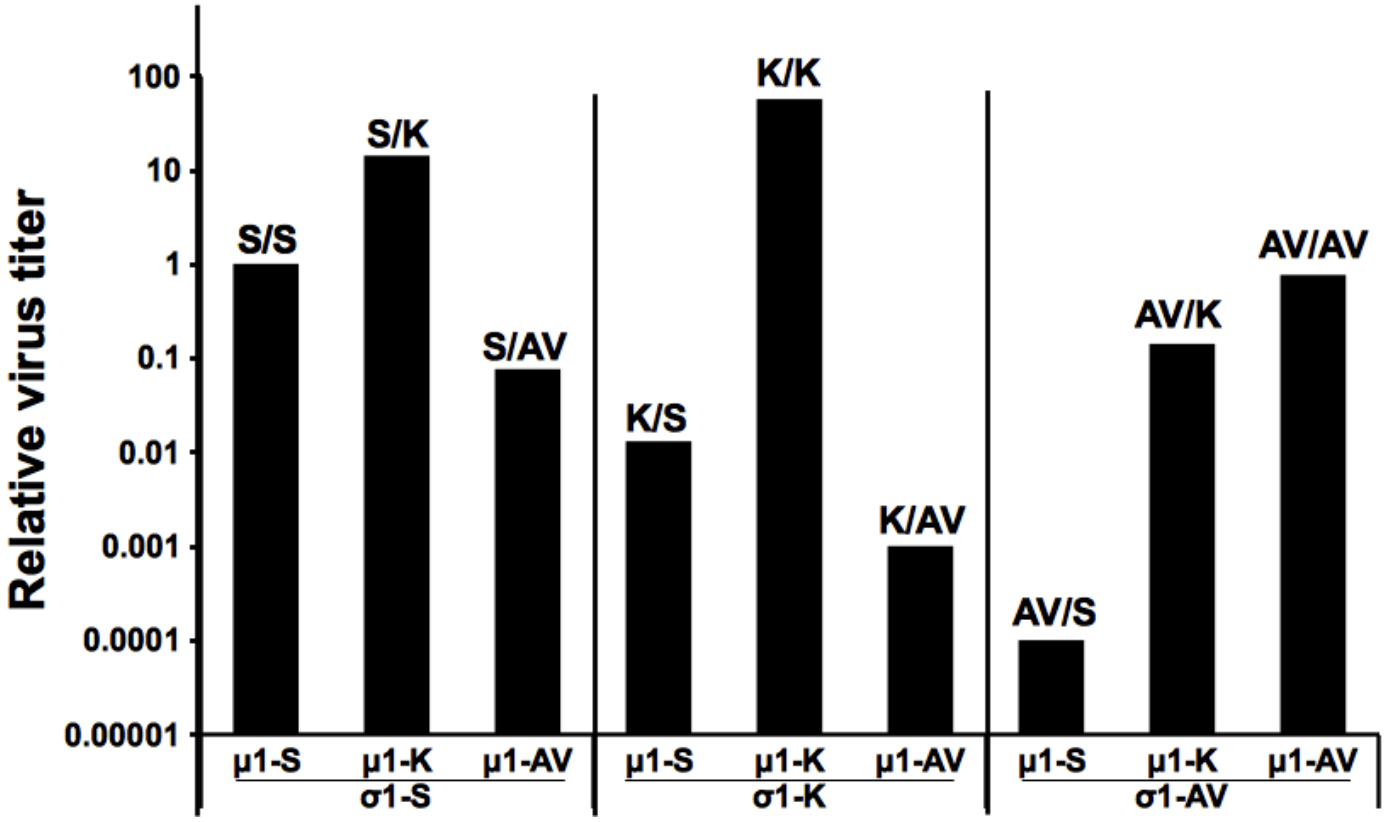
Relative virus titer
100
10
1
0.1
0.01
0.001
0.0001
0.00001
S/S
S/K
S/AV
K/S
K/K
K/AV
AV/S
AV/K
AV/AV
μ1-S
μ1-K
μ1-AV
σ1-S
σ1-K
σ1-AV

Figure 5

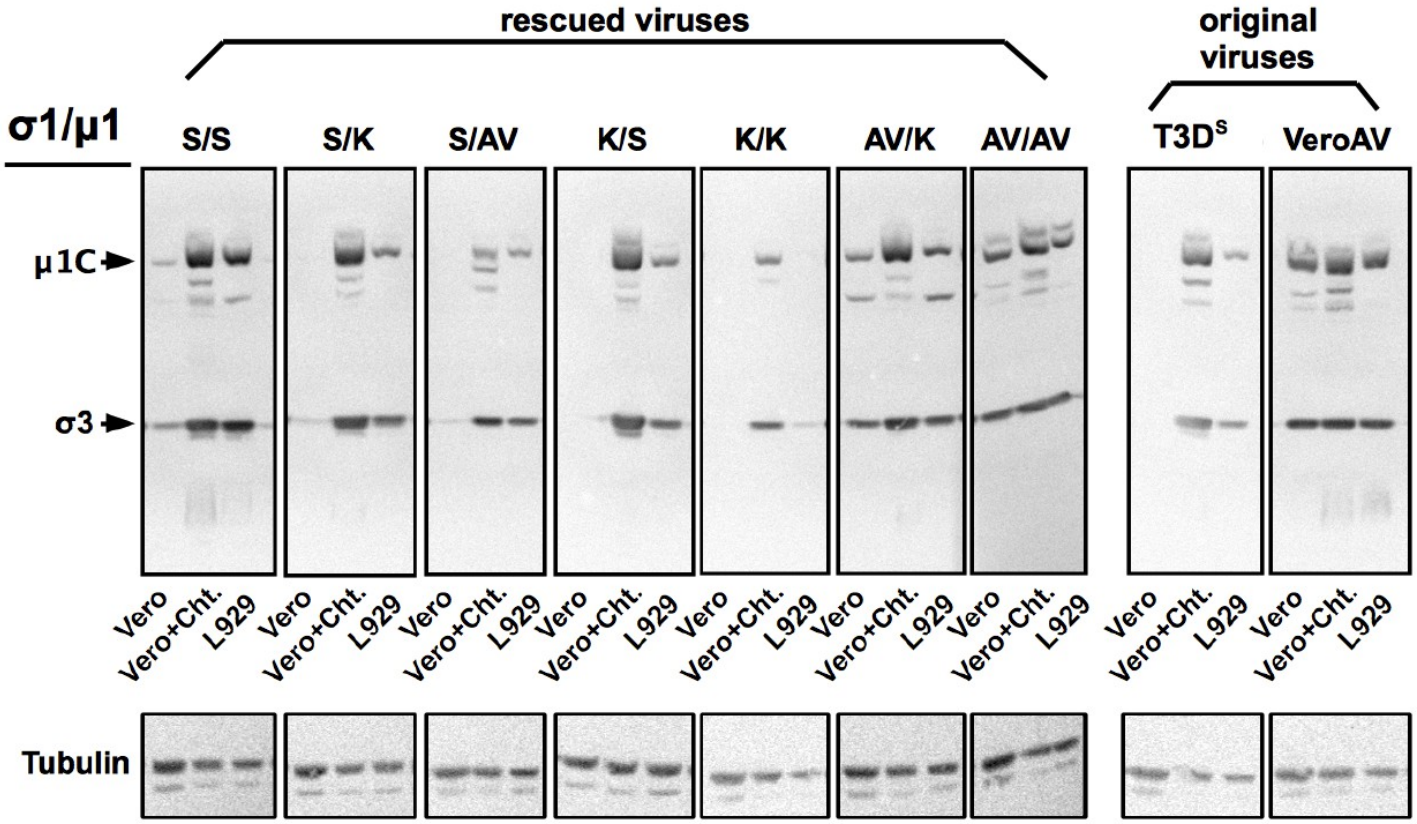
rescued viruses
original viruses
σ1/μ1
S/S
S/K
S/AV
K/S
K/K
AV/K
AV/AV
T3D^S
VeroAV
μ1C
σ3
Vero
Vero+Cht.
L929
Tubulin

Figure 6

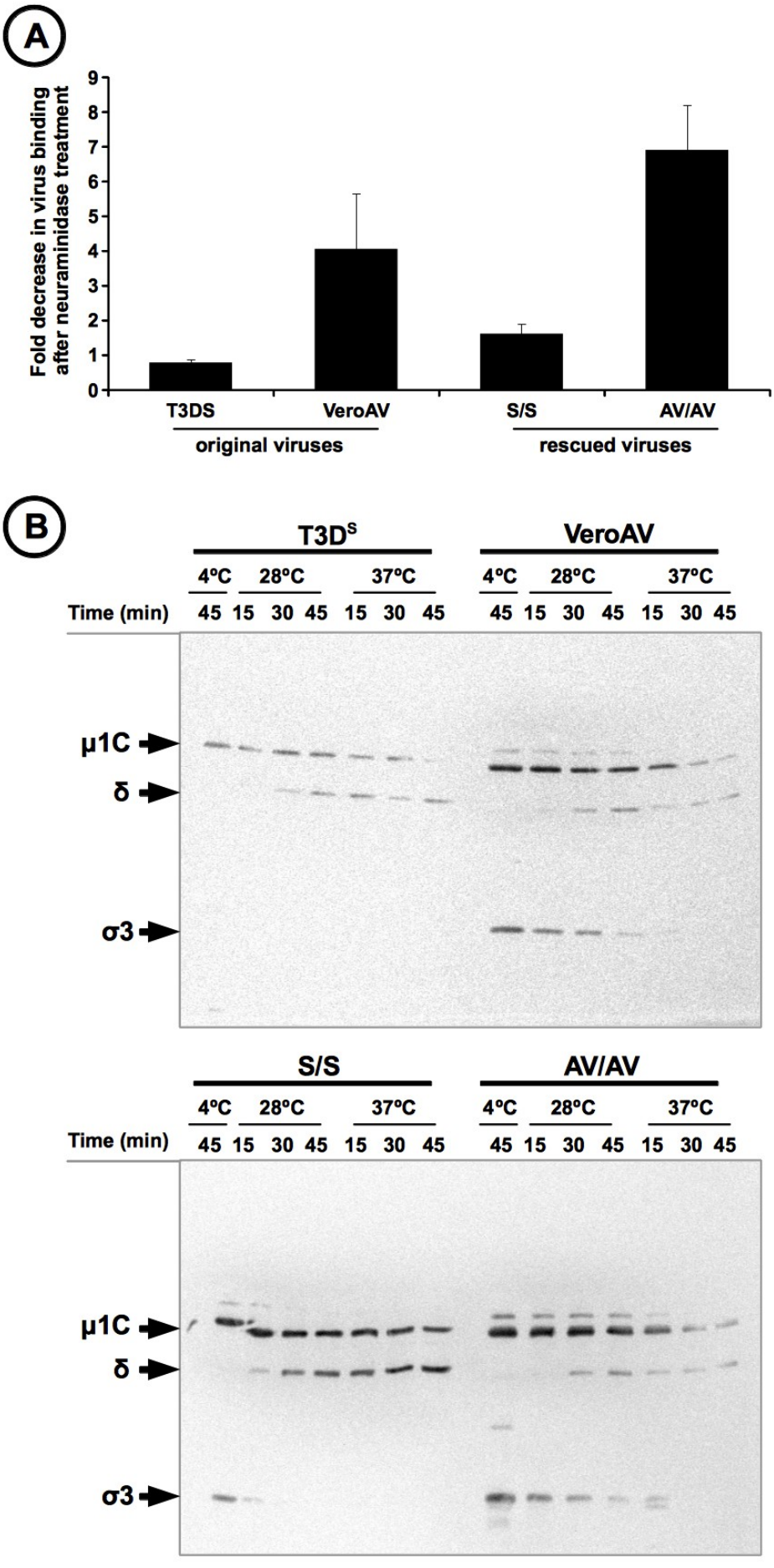
A
Fold decrease in virus binding after neuraminidase treatment
0
1
2
3
4
5
6
7
8
9
T3DS
VeroAV
S/S
AV/AV
original viruses
rescued viruses
B
T3D^S
VeroAV
4ºC
28ºC
37ºC
Time (min)
45 15 30 45 15 30 45
μ1C
δ
σ3
S/S
AV/AV

Figure 7

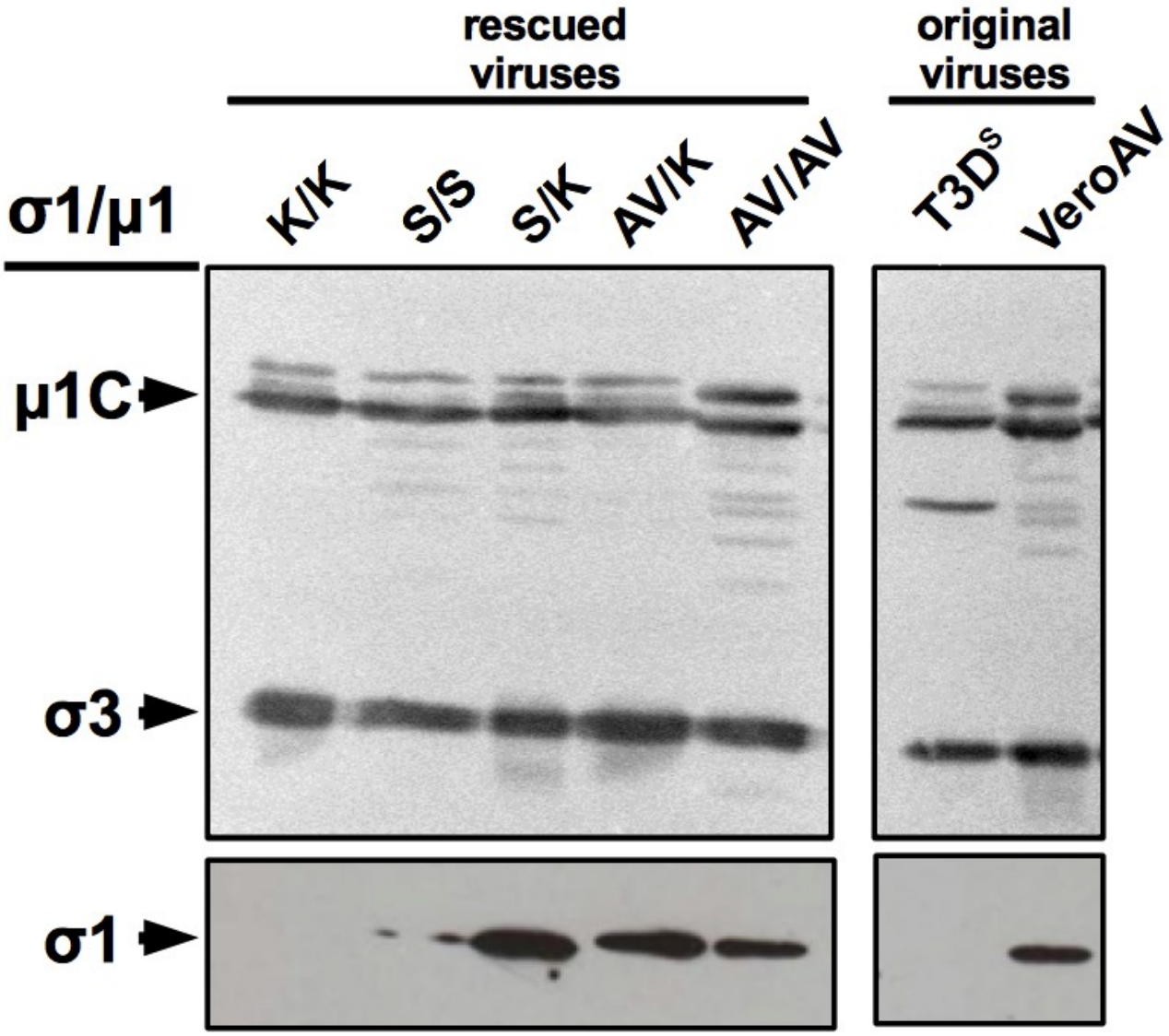
rescued viruses
original viruses
σ1/μ1
K/K
S/S
S/K
AV/K
AV/AV
T3D^S
VeroAV
μ1C
σ3
σ1

Supplementary Figure 1